



UNITED STATES PATENT AND TRADEMARK OFFICE

UNITED STATES DEPARTMENT OF COMMERCE  
United States Patent and Trademark Office  
Address: COMMISSIONER FOR PATENTS  
P.O. Box 1450  
Alexandria, Virginia 22313-1450  
www.uspto.gov

*TPW*

APPLICATION NO.	FILING DATE	FIRST NAMED INVENTOR	ATTORNEY DOCKET NO.	CONFIRMATION NO.
-----------------	-------------	----------------------	---------------------	------------------

10/802,762

03/18/2004

Dong Soo Lee

122988-05007285

4699

43569 7590 07/26/2007  
MAYER, BROWN, ROWE & MAW LLP  
1909 K STREET, N.W.  
WASHINGTON, DC 20006

EXAMINER

LIN, PHYOWAI

ART UNIT

PAPER NUMBER

2613

MAIL DATE

DELIVERY MODE

07/26/2007

PAPER

Please find below and/or attached an Office communication concerning this application or proceeding.

The time period for reply, if any, is set in the attached communication.

## Office Action Summary

Application No.

10/802,762

Applicant(s)

LEE ET AL.

Examiner

PHYOWAI LIN

Art Unit

2613

-- The MAILING DATE of this communication appears on the cover sheet with the correspondence address --

### Period for Reply

A SHORTENED STATUTORY PERIOD FOR REPLY IS SET TO EXPIRE 3 MONTH(S) OR THIRTY (30) DAYS, WHICHEVER IS LONGER, FROM THE MAILING DATE OF THIS COMMUNICATION.

- Extensions of time may be available under the provisions of 37 CFR 1.136(a). In no event, however, may a reply be timely filed after SIX (6) MONTHS from the mailing date of this communication.
- If NO period for reply is specified above, the maximum statutory period will apply and will expire SIX (6) MONTHS from the mailing date of this communication.
- Failure to reply within the set or extended period for reply will, by statute, cause the application to become ABANDONED (35 U.S.C. § 133). Any reply received by the Office later than three months after the mailing date of this communication, even if timely filed, may reduce any earned patent term adjustment. See 37 CFR 1.704(b).

### Status

- 1) ☐ Responsive to communication(s) filed on \_\_\_\_.
- 2a) ☐ This action is **FINAL**. 2b) ☒ This action is non-final.
- 3) ☐ Since this application is in condition for allowance except for formal matters, prosecution as to the merits is closed in accordance with the practice under *Ex parte Quayle*, 1935 C.D. 11, 453 O.G. 213.

### Disposition of Claims

- 4) ☒ Claim(s) 1-5 is/are pending in the application.
- 4a) Of the above claim(s) \_\_\_\_ is/are withdrawn from consideration.
- 5) ☐ Claim(s) \_\_\_\_ is/are allowed.
- 6) ☒ Claim(s) 1-5 is/are rejected.
- 7) ☐ Claim(s) \_\_\_\_ is/are objected to.
- 8) ☐ Claim(s) \_\_\_\_ are subject to restriction and/or election requirement.

### Application Papers

- 9) ☐ The specification is objected to by the Examiner.
- 10) ☐ The drawing(s) filed on \_\_\_\_ is/are: a) ☐ accepted or b) ☐ objected to by the Examiner.  
Applicant may not request that any objection to the drawing(s) be held in abeyance. See 37 CFR 1.85(a).  
Replacement drawing sheet(s) including the correction is required if the drawing(s) is objected to. See 37 CFR 1.121(d).
- 11) ☐ The oath or declaration is objected to by the Examiner. Note the attached Office Action or form PTO-152.

### Priority under 35 U.S.C. § 119

- 12) ☐ Acknowledgment is made of a claim for foreign priority under 35 U.S.C. § 119(a)-(d) or (f).
- a) ☐ All b) ☐ Some \* c) ☐ None of:
- ☐ Certified copies of the priority documents have been received.
  - ☐ Certified copies of the priority documents have been received in Application No. \_\_\_\_.
  - ☐ Copies of the certified copies of the priority documents have been received in this National Stage application from the International Bureau (PCT Rule 17.2(a)).

\* See the attached detailed Office action for a list of the certified copies not received.

### Attachment(s)

- 1) ☒ Notice of References Cited (PTO-892)
- 2) ☐ Notice of Draftsperson's Patent Drawing Review (PTO-948)
- 3) ☐ Information Disclosure Statement(s) (PTO/SB/08)  
Paper No(s)/Mail Date \_\_\_\_.
- 4) ☐ Interview Summary (PTO-413)  
Paper No(s)/Mail Date. \_\_\_\_.
- 5) ☐ Notice of Informal Patent Application
- 6) ☐ Other: \_\_\_\_.

Art Unit: 2613

## DETAILED ACTION

### ***Claim Rejections - 35 USC § 103***

1. The following is a quotation of 35 U.S.C. 103(a) which forms the basis for all obviousness rejections set forth in this Office action:

(a) A patent may not be obtained though the invention is not identically disclosed or described as set forth in section 102 of this title, if the differences between the subject matter sought to be patented and the prior art are such that the subject matter as a whole would have been obvious at the time the invention was made to a person having ordinary skill in the art to which said subject matter pertains. Patentability shall not be negated by the manner in which the invention was made.

2. **Claims 1-5** are rejected under 35 U.S.C. 103(a) as being unpatentable over Yutaka et al., "Novel Modulation and Detection for Bandwidth-Reduced RZ Formats Using Duobinary-Mode Splitting in Wideband PSK/ASK Conversion" @2002 IEEE in view of F. Liu et al., "A novel chirped return-to-zero transmitter and transmission experiments," European Conference on Optical Communication 2000, Munich, Germany, Vol. 3, pp. 113-114, Sept 3 - 7 2000.

**Regarding to claim 1**, Yutaka et al. disclose an apparatus for generating a Carrier-Suppressed Return-to-Zero (CS-RZ) signal (see FIG.3), comprising:

a mixer generating a modulator input by mixing data (NRZ data signal) with a half clock signal (B/2 clock) (see FIG.3);

a Low Pass Filter (LPF) band-limiting the modulator input data, which has been provided from the mixer, into low frequency band data (see page 2068, right column lines 27-31 and FIG.3 where in the modulator input data is filtered by LPF into low frequency band data);

a driver amplifier amplifying the modulator input data generated by the mixing of the mixer and the band-limiting of the LPF (see page 2068, right column lines 27-31 and FIG.3 where in the modulator input data is boosted by amplifier for amplifying the input data signal) ; and

an external modulator (MZ modulator) generating a CS-RZ signal, in which phases of adjacent pulses are inverted, by applying bias voltage to the modulator input data, which has been amplified by the driver amplifier, to be placed at a null point of a transfer function of the external modulator (see page 2068, right column lines 4-10, lines 12-15 and FIG.3 where in a push-pull type Mach-Zehnder modulator can generate duobinary CS-RZ signal with phases are inverted by applying bias voltage to the modulator at the transmission null point).

In FIG.3 of Yutaka et al. the LPF is after the amplifier; but the LPF of the applicant is before the amplifier. However, such limitation is merely a matter of design choice and would have been obvious in the system of Yutaka et al. Since LPF is functioning for filtering out as low frequency band data, the LPF can be installed before or after the amplifier and both position are functionally equivalent. Therefore, to install the LPF before or after the amplifier would have been a matter of obvious design choice to one of the ordinary skill in the art.

Even though, Yutaka et al. disclose that an NRZ data signal from the optical duobinary data modulator drives the modulator MZ#2 and a half clock signal from two-mode-beat pulse generator drives the modulator MZ#1 respectively. Yutaka et al. fail to specifically disclose a mixer to mix the NRZ data signal with the half clock signal and couple the two signals into a single Mach-Zehnder modulator with CW light input.

However F. Liu et al. in the same field of endeavor, disclose a system in which a mixer (2:1 selector see FIG.1) is used to mix the NRZ data signal with clock signal. After mixing the two signals, then the mixed signal is coupled into the single MZ modulator with CW light input (see FIG.1).

By mixing the NRZ data signal with clock signal into the 2:1 selector and using a single MZ modulator instead of two MZ modulators, F. Liu et al. provide a cost effective system and low losses in the transmission system.

Therefore, it would have been obvious to one of the ordinary skill in the art at the time invention was made to use the 2:1 selector to mix the NRZ data signal and half clock signal and coupling the mixing signals into the single MZ modulator as taught by F. Liu et al. to generate the duobinary CS-RZ signal so that a cost-effective and low losses system can be achieved.

**Regarding to claim 2**, Yutaka et al. and F. Liu et al. disclose everything claimed as applied above (see claim 1). In addition, F.Liu et al. disclose wherein the mixer (2:1 selector) adjusts logical data "0" to data 0 V and adjusts a clock signal to symmetrically swing around 0 V (see paragraph under title Structure of the CRZ transmitter: lines 6-8 where in the 2:1 selector controls the data signal to 0 V (falling edge) and clock signal to swing around 0 V (rising edge)).

Therefore it would have been obvious to one of the ordinary skill in the art at the time invention was made to use the 2:1 selector to control the NRZ data signal and clock signal into particular voltage range because it would allow to have accurate and useful design choice for mixture output before coupling into an modulator for modulation.

**Regarding to claim 3**, Yutaka et al. and F. Liu et al. disclose everything claimed as applied above (see claim 1). In addition, Yutaka et al. disclose wherein: the band limiting reduces an optical spectrum bandwidth of the CS-RZ signal while reducing noise of the signal; the decrease of the optical spectrum bandwidth improves dispersion characteristics of the optical signal; and the bandwidth of the LPF is adjusted to increase dispersion tolerance of the optical signal while minimizing distortion of the optical signal (see Abstract, lines 14-20 and see FIG.3 where in using filter (LPF) in generating duobinary CS-RZ signal system can achieve reducing the bandwidth of optical spectrum so that minimizing distortion of the optical signal as well as increase dispersion tolerance of optical signal).

Art Unit: 2613

**Regarding to claim 4**, Yutaka et al. and F. Liu et al. disclose everything claimed as applied above (see claim 1). In addition, Yutaka et al. disclose wherein the driver amplifier performs amplification so that logical data "0" becomes 0 V and logical data "1" becomes.  $\pm V_{pi}$ . (see FIG.3 and FIG.4 (b) where in the amplifier amplifies the NRZ data signal as making the logical data 0 and 1 as 0 and  $\pm V_{pi}$ ).

**Regarding to claim 5**, Yutaka et al. and F. Liu et al. disclose everything claimed as applied above (see claim 1). In addition, Yutaka et al. disclose wherein the LPF is an electrical filter designed to reduce the spectrum of the optical signal and improve the dispersion characteristics of the optical signal (see Abstract, lines 14-20 and see FIG.3 where in using filter (LPF) in generating duobinary CS-RZ signal system can achieve reducing the bandwidth of optical spectrum so that minimizing distortion of the optical signal as well as increase dispersion tolerance of optical signal).

#### ***Citation of Pertinent Prior Art***

3. The prior art made of record and not relied upon is considered pertinent to applicant's disclosure.

Hayee et al. (US Patent Number 6980746) disclose the system for generating CS-RZ signal by mixing data and half clock signal with single modulator.

***Response to Arguments***

4. Applicant's arguments with respect to claims 1-5 have been considered but are moot in view of the new ground of rejection.

***Conclusion***

5. Any inquiry concerning this communication or earlier communications from the examiner should be directed to PHYOWAI LIN whose telephone number is (571) 270-1659. The examiner can normally be reached on Monday through Friday.

If attempts to reach the examiner by telephone are unsuccessful, the examiner's supervisor, Kenneth Vanderpuye can be reached on (571) 272-3078. The fax phone number for the organization where this application or proceeding is assigned is 571-273-8300.

Information regarding the status of an application may be obtained from the Patent Application Information Retrieval (PAIR) system. Status information for published applications may be obtained from either Private PAIR or Public PAIR. Status information for unpublished applications is available through Private PAIR only. For more information about the PAIR system, see <http://pair-direct.uspto.gov>. Should you have questions on access to the Private PAIR system, contact the Electronic Business Center (EBC) at 866-217-9197 (toll-free). If you would like assistance from a USPTO Customer Service Representative or access to the automated information system, call 800-786-9199 (IN USA OR CANADA) or 571-272-1000.

PWL

07/19/07

  
**KENNETH VANDERPUYE**  
**SUPERVISORY PATENT EXAMINER**



**Notice of References Cited**Application/Control No.  
10/802,762Applicant(s)/Patent Under  
Reexamination  
LEE ET AL.Examiner  
PHYOWAI LINArt Unit  
2613

Page 1 of 1

**U.S. PATENT DOCUMENTS**

*		Document Number Country Code-Number-Kind Code	Date MM-YYYY	Name	Classification
*	A	US-6,980,746	12-2005	Hayee, M. Imran	398/183
*	B	US-7,116,917	10-2006	Miyamoto et al.	398/185
	C	US-			
	D	US-			
	E	US-			
	F	US-			
	G	US-			
	H	US-			
	I	US-			
	J	US-			
	K	US-			
	L	US-			
	M	US-			

**FOREIGN PATENT DOCUMENTS**

*		Document Number Country Code-Number-Kind Code	Date MM-YYYY	Country	Name	Classification
	N					
	O					
	P					
	Q					
	R					
	S					
	T					

**NON-PATENT DOCUMENTS**

*		Include as applicable: Author, Title Date, Publisher, Edition or Volume, Pertinent Pages)
	U	Yutaka et al: " Novel Modulation and Detection for Bandwidth-Reduced RZ Formats Using Duobinary-Mode Splitting in Wideband PSK/ASK Conversion" @2002 IEEE.
	V	F. Liu et al., "A novel chirped return-to-zero transmitter and transmission experiments," European Conference on Optical Communication 2000, Munich, Germany, Vol. 3, pp. 113-114, Sept 3 - 7 2000.
	W	
	X	

\*A copy of this reference is not being furnished with this Office action. (See MPEP § 707.05(a).)  
Dates in MM-YYYY format are publication dates. Classifications may be US or foreign.

# Novel Modulation and Detection for Bandwidth-Reduced RZ Formats Using Duobinary-Mode Splitting in Wideband PSK/ASK Conversion

Yutaka Miyamoto, *Member, IEEE*, Akira Hirano, Shoichiro Kuwahara, Masahito Tomizawa, *Member, IEEE*, and Yasuhiko Tada

**Abstract**—This paper proposes a novel duobinary-mode-splitting scheme that uses wideband phase-shift-keying (PSK)/amplitude-shift-keying (ASK) conversion for modulation and detection of bandwidth-reduced return-to-zero (RZ) modulation formats. We have first demonstrated that the proposed scheme greatly simplifies the modulation process of the duobinary carrier-suppressed RZ format (DCS-RZ) based on baseband binary nonreturn-to-zero (NRZ) modulation. We also proposed carrier-suppressed RZ differential-phase-shift-keying format (CS-RZ DPSK) as a novel bandwidth-reduced RZ format by applying the proposed scheme in the detection process. These novel RZ formats are shown to be very useful for dense wavelength-division multiplexed (DWDM) transport systems using high-speed channels, over 40 Gb/s, with spectrum efficiencies higher than 0.4 b/s/Hz. We demonstrate that the proposed modulation and detection scheme greatly simplifies the DWDM transmitter and receiver configuration if the periodicity of the optical PSK/ASK conversion filter equals the WDM channel spacing. The large tolerance of the formats against several fiber nonlinearities and their wide dispersion tolerance characteristics are tested at the channel rate of 43 Gb/s with 100-GHz spacing. The novel CS-RZ DPSK format offers higher nonlinearity tolerance against cross-phase modulation than does the DCS-RZ format.

**Index Terms**—Fiber optics communication, modulation.

## I. INTRODUCTION

HIGH CAPACITY wavelength-division-multiplexing (WDM) transport systems with channel rates exceeding 40 Gb/s are attractive: they offer high capacity over multiterabit-per-second capacity with fewer channels and therefore attain high signal spectrum efficiency, especially in dense wavelength-division multiplexed (DWDM) systems with a spectral efficiency exceeding 0.4 b/s/Hz. Since the modulation bandwidth and the channel spacing are comparable in such DWDM systems, the choice of the signal format is a key issue in minimizing the channel crosstalk penalty. The required features placed on modulation format are

- compact modulation spectrum;
- simple configuration of transmitter and receiver;
- high fiber-nonlinearity tolerance.

Narrower optical modulation bandwidth is desirable, especially when considering the line rate increase by the introduction of forward error correction (FEC). Compact modulation bandwidth is also desirable to enlarge several dispersion-tolerance characteristics, such as group velocity dispersion (GVD) and polarization-mode dispersion (PMD), when considering channel speed of more than 40 Gb/s. Optical duobinary format [1] and optical modified duobinary format [2] based on partial-response signals are very attractive, because their optical modulation bandwidth can be compressed to the data bit rate  $B$ , that is, the half-bandwidth of the nonreturn-to-zero (NRZ) format ( $2B$ ).

A simple direct-detection receiver can be used in these formats, which is also desirable for cost-effective realization for the receivers. In the transmitter configuration, on the other hand, the conventional duobinary systems require broad-band baseband analog processing to generate three-level partial response signals, which makes it difficult to realize high-speed operation. The intersymbol interference (ISI) in the initial output waveforms of duobinary systems are inherently larger than conventional NRZ formats; therefore, the receiver sensitivity is degraded. Since these formats have pattern-dependent pulsewidth, fiber nonlinearity, such as self-phase modulation (SPM) and cross-phase modulation (XPM), tend to increase the pattern-dependent ISI which degrades the transmission performance at data rates over 40 Gb/s [3].

The return-to-zero (RZ) format, on the other hand, has small initial ISI in its output waveform and high fiber nonlinear tolerance because of the pattern-independent pulsewidth. For this reason, several RZ formats are adopted in long-distance transmission systems. However, since the conventional RZ format uses the three-mode-locked mode, as shown in Fig. 1, it requires twice the bandwidth of an NRZ signal (namely,  $> 4B$ , where  $B$  is the line rate). The crosstalk penalty of the conventional RZ format would be increased for comparable modulation bandwidth and channel spacing (e.g., 100-GHz spacing in 40 Gb/s channel transmission). In addition, the conventional RZ format offers much smaller GVD tolerance than does the NRZ format because of its large modulation bandwidth. It is strongly demanded to overcome the transmission distance limitation induced by both the dispersion characteristics and the fiber nonlinearities in such a DWDM systems. Simple transmitter and

Manuscript received June 3, 2002; revised September 19, 2002.

The authors are with NTT Network Innovation Laboratories, NTT Corporation, Kanagawa 239-0847, Japan (e-mail: miyamoto@exa.onlab.ntt.co.jp).  
Digital Object Identifier 10.1109/JLT.2002.806749

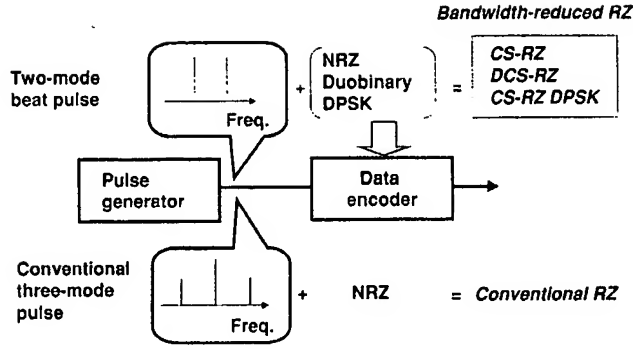


Fig. 1. Bandwidth reduction of RZ format using phase modulation.

receiver configurations are also important for the cost-effective realization of such high-capacity WDM optical transport networks.

To overcome these issues, we have proposed bandwidth reduction schemes for the RZ format by using phase modulation with phase reversal, both in the pulse-generation process and data-modulation process, as shown in Fig. 1 [3]. Fig. 2 shows the modulation spectra of proposed bandwidth reduced-bandwidth RZ formats; the carrier-suppressed RZ (CS-RZ) format [4] [5] and the duobinary carrier suppressed RZ (DCS-RZ) format [6], [7]. Fig. 2 shows the measured 40-Gb/s modulation spectra of these formats [3]. Compared with the conventional RZ format, the CS-RZ and DCS-RZ formats can enhance the fiber-nonlinear tolerance of DWDM systems and reduce the modulation bandwidth,  $3B$  and  $2B$ , respectively. The DCS-RZ format is especially attractive, because it has the same modulation bandwidth ( $2B$ ) as the NRZ format, and it is the narrowest, to our knowledge, of all the RZ formats. However, the conventional transmitter configuration for the DCS-RZ format is also not suitable for ultrahigh-speed operation over 40 Gb/s due to the complicated baseband analog processing used in the data-modulation process of optical duobinary format.

This paper proposes a novel duobinary-mode-splitting scheme using wideband analog processing in optical carrier frequency based on wideband PSK/ASK that simplifies the transmitter configuration of DCS-RZ formats for the high-bit-rate channel DWDM transmission systems [8] and creates the novel CS-RZ DPSK format [9] with a simple detection configuration. Section II describes the features and issues of the conventional DCS-RZ format. We then describe the novel idea of the duobinary-mode splitting of the DPSK signal that is applied to a new modulation scheme of DCS-RZ format using a wideband PSK/ASK conversion filter. We also base a detection scheme on duobinary-mode-splitting to create CS-RZ DPSK as a novel bandwidth-reduced RZ format. We upgrade these modulation and detection schemes to the DWDM transmission system, which greatly simplifies the transmitter and receiver configurations. Sections III demonstrates the experimental results gained in 100-GHz-spaced  $N \times 43$  Gb/s DWDM transmission using the proposed DCS-RZ and CS-RZ DPSK formats. Section IV provides a performance comparison of the DCS-RZ and CS-RZ DPSK formats for 43-Gb/s/channel WDM transmission over dispersion-shifted fiber. Our conclusions are given in Section V.

## II. PRINCIPLE

### A. Feature and Issue of the Conventional DCS-RZ Transmission System

The conventional transmission system using DCS-RZ format is shown in Fig. 3. The DCS-RZ signal transmitter shown in Fig. 3 consists of a two-mode-beat pulse generator and an optical duobinary data modulator [6].

In the pulse generation section, the optical carrier signal is modulated by a push-pull type Mach-Zehnder (MZ#1) modulator biased at the transmission null point. Two pairs of half-line-rate clock signals, synchronized to the transmission data, are fed to each electrode of the MZ modulator. Using the phase encoding characteristic and frequency doubling characteristic of the MZ modulator, a two-mode beat pulse train with alternate  $\pi$  phase flip is generated at point *a* in Fig. 3: the beat frequency equal to the line rate  $B$ . The waveform of the two mode beat pulse  $c(t)$  and its signal spectrum  $P_{2mode}(\omega)$  are given by formula (1);

$$c(t) = \exp[-j(\omega_c - \omega_b/2)t] + \exp[-j(\omega_c + \omega_b/2)t] \\ = \cos(\omega_b t/2) \times \exp[-j\omega_c t] \quad (1-1)$$

$$P_{2mode}(\omega) = 2\pi\delta(\omega - \omega_c + \omega_b/2) + 2\pi\delta(\omega - \omega_c - \omega_b/2) \quad (1-2)$$

where  $\omega_c$  and  $\omega_b (=2\pi B)$  are angular frequency of optical carrier signal and data bit rate frequency, respectively, and  $\delta(\omega)$  is delta function.

In the data modulation section, the input electrical NRZ signal is converted into precoded NRZ signal by digital precoder circuit (shown as solid square in Fig. 3) consisting of an exclusive OR and a one bit delay circuit. The logic in the precoded output signal is inverted for every mark bit in input NRZ signals. The electrical complementary precoded NRZ signals are boosted and converted into complementary three-level electrical duobinary signals by Bessel-Thomson-type low pass filters (LPF) known as duobinary filters. The transfer function of baseband duobinary filter is given by formula (2)

$$H(\omega) = 2T \cos(\omega T/2) \quad / \omega / < \pi/T \quad (2-1)$$

$$H(\omega) = 0 \quad / \omega / > \pi/T. \quad (2-2)$$

The complementary duobinary signals are fed to a push-pull type MZ modulator (MZ#2) biased at transmission null point. Power spectrum of the optical duobinary signal  $P_{duo}(\omega)$  for the rectangular shaped NRZ signal input [1] is given by formula (3)

$$P_{duo}(\omega) = T \sin^2((\omega - \omega_c)T) / ((\omega - \omega_c)T)^2. \quad (3)$$

Since the two longitudinal beat modes of the two mode beat given by (1) are modulated by the optical duobinary signal, a twin duobinary signal spectrum separated by the line rate frequency is observed as shown in Fig. 2(c). The power spectrum of DCS-RZ format  $P_{DCS-RZ}(\omega)$  was approximately given by formula (5) if the high-order spectrum components of duobinary signal is omitted. Using formula (1) and (2)

$$P_{DCS-RZ}(\omega) = 4\omega^2 \sin^2(\omega T) / ((\omega - \omega_c)^2 - (\omega_b/2)^2)^2 \quad (4)$$

$$\sim P_{duo}(\omega - \omega_c - \omega_b/2) + P_{duo}(\omega - \omega_c + \omega_b/2). \quad (5)$$

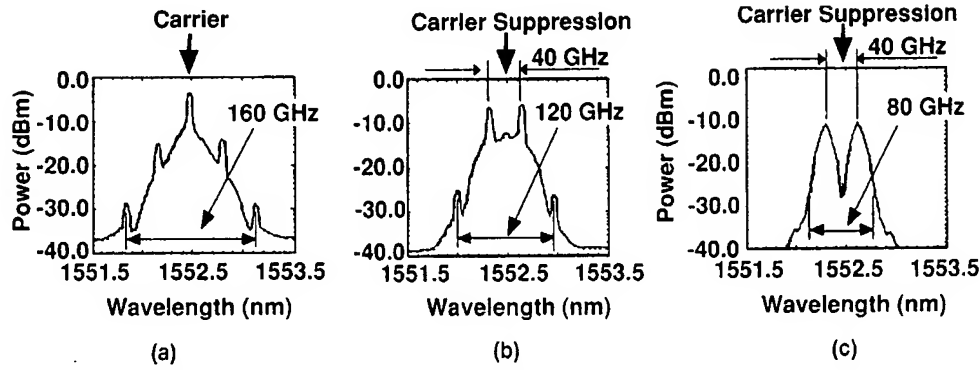


Fig. 2. The measured 40-Gb/s modulation spectra. (a) Conventional RZ. (b) CS-RZ. (c) DCS-RZ.

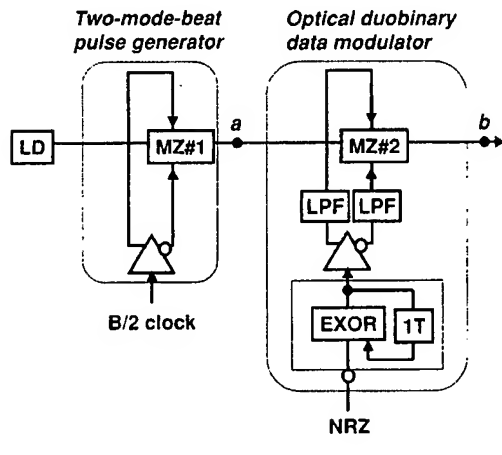


Fig. 3. Conventional transmitter configuration of DCS-RZ format. (a) DCS-RZ format using two-mode beat pulse. (b) DCS-RZ format using differential baseband signals.

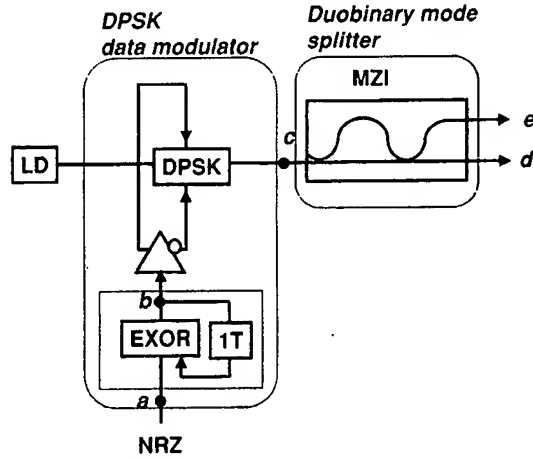


Fig. 5. Novel configuration of DCS-RZ transmitter using duobinary mode splitting of DPSK signal.

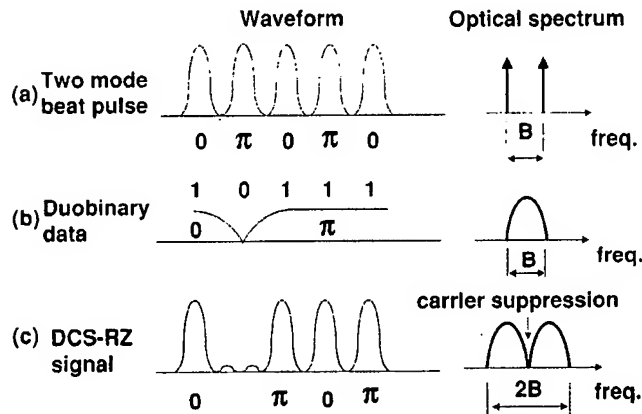


Fig. 4. The operation of DCS-RZ signal transmitter. (a) Waveform and spectra of two mode beat pulse. (b) Waveform and spectra of optical duobinary format. (c) Waveform and spectra of DCS-RZ format.

Fig. 4 shows the waveform response and modulation spectra at several interface of DCS-RZ transmitter. Fig. 4(a) shows the waveform response and pulse spectra of two mode beat pulse at the output of MZ modulator (MZ#1) in Fig. 3. Two longitudinal modes whose mode spacing is equal to the bit rate appear with carrier suppression. According to the formula (1), its waveform is sinusoidal clock pulse with alternate bit phase reversal at a repetition frequency equal to the line rate. Fig. 4(b) shows the wave-

form response and modulation spectra of duobinary format. As shown in Fig. 4(b) the waveform of optical duobinary signal has large ISI at the space level. The modulation bandwidth is compressed to line rate  $B$ . Fig. 4(c) shows the waveform response of DCS-RZ signal that is given by the product of two-mode-beat signal  $c(t)$  and duobinary signal  $d(t)$ . DCS-RZ format is a constant-pulsewidth RZ signal. It also greatly reduces the ISI at the space level compared with duobinary format. Note that DCS-RZ has the phase encoding rule of alternate-mark-bit phase reversal which is different from CS-RZ format. As shown in Fig. 4(c), the modulation bandwidth of the DCS-RZ signal is twice the line rate ( $2B$ ), which is as narrow as that of the NRZ signal. This feature enables high signal spectral efficiency, over 0.4 b/s/Hz, with large power margin [3]. The conventional DCS-RZ transmitter, however, requires complicated broadband baseband analog signal processing in data modulation section that prevents increasing the line rate over 40 Gb/s.

#### B. DCS-RZ Transmission System Using Duobinary-Mode Splitting of DPSK

To solve this problem, we propose novel DCS-RZ signal generation by the duobinary-mode splitting of the DPSK signal format in a PSK/ASK conversion filter.

Fig. 5 shows the operation of the proposed DCS-RZ transmitter. The transmitter consists of a DPSK data modulator complementarily driven by simple NRZ signals from a precoder

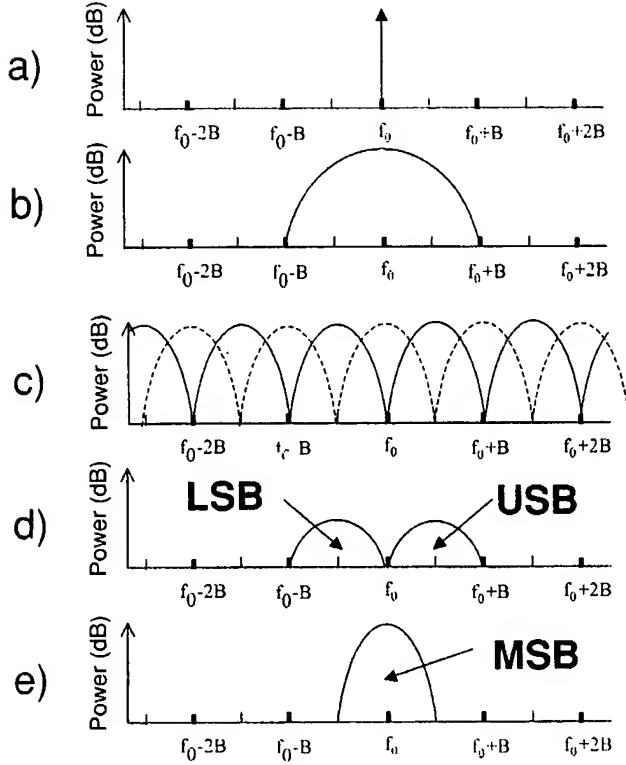


Fig. 6. Proposed DCS-RZ signal modulation. (a) Spectra of LD output. (b) Modulation spectra of DPSK signal. (c) Transmission characteristic of duobinary-mode-splitting filter. (d) Spectral structure of DCS-RZ signal split from DPSK signal. (e) Spectral structure of duobinary signal split from DPSK signal.

circuit, and a Mach Zehnder Interferometer (MZI) filter as a PSK/ASK converter. The input data signal NRZ data signal at point *a* in Fig. 5 is converted into a precoded binary NRZ data signal at point *b* in Fig. 5. The precoder circuit in Fig. 5 is different from that in Fig. 3 in term of an inverter at the input port. The precoded NRZ signal is boosted and is fed to push-pull MZ modulator biased at transmission null point. Under this configuration, the carrier signal from the LD is modulated with a DPSK format at point *c* in Fig. 5, whose modulations spectra is shown in Fig. 6(b). Fig. 6(c) shows the transmission characteristics of the MZI filter in the through port (point *d* in Fig. 5) and the cross port (point *e* in Fig. 5). Using the MZI filter whose free spectral range (FSR) is equal to the line rate, the DPSK signal is spectrally split into three duobinary components as shown in Fig. 6(d) and (e): LSB (Lower side band)-duobinary mode, MSB (Middle side band)-duobinary mode, and USB (Upper side band)-duobinary mode. Transfer function of MZI filter of through port and cross port are given by (6-1) and (6-2), respectively;

$$H(\omega) = 2T \cos((\omega - \omega_c)T/2) \quad (6-1)$$

$$H(\omega) = 2T \sin((\omega - \omega_c)T/2). \quad (6-2)$$

Since the optical MZI filter has the same periodic transfer function as duobinary filter given by formula (2) at the carrier frequency, the DPSK signal modulated by rectangular shape NRZ data signal is converted to the optical duobinary signal.

The logics of the LSB mode and USB mode are the same, and they are opposite to that of the MSB mode. The solid trans-

mission characteristic of the MZI-filter port yields the LSB and USB duobinary modes, whose frequency spacing equals the line rate  $B$  of the DPSK signal. Since the LSB and USB duobinary modes, which are split from the DPSK signal, are mode locked, these twin duobinary modes can be combined to form a DCS-RZ signal. Note that the spectral shape of DCS-RZ generated by this scheme is strongly affected by the power spectrum of input DPSK signal, pulsewidth depend on input data pattern that induce some jitter in rising edge and falling in its waveform [7]. The dotted transmission characteristic of the MZI-filter port, on the other hand, splits the MSB duobinary mode to yield a duobinary signal. Since only simple NRZ signals are used for baseband signal processing (complicated three-level signals are not used), this DCS-RZ transmitter configuration is very simple and suitable for ultra-high speed operation.

The duobinary mode splitting of 43 Gb/s DPSK was experimentally confirmed by using a narrow bandpass filter and an MZI filter, both of which were temperature tuned. The 43 Gb/s eye openings of the USB and MSB duobinary modes are as shown in Fig. 7. The USB duobinary mode was confirmed to have reverse logic compared to the MSB duobinary mode by measuring their bit errors. The 43-Gb/s DCS-RZ shown in Fig. 7(d) was obtained using a 100 GHz MZI filter. Therefore, the DCS-RZ signal can be obtained by duobinary mode splitting a DPSK signal in PSK/ASK conversion.

Fig. 8 shows the WDM upgrade of the proposed transmitter configuration shown in Fig. 5 using the periodic transfer function of MZI filter in optical carrier frequency. When the WDM channel spacing is equal to a multiple of the FSR of the MZI filter, the WDM DPSK signal can be converted into a WDM DCS-RZ signal by using a single MZI filter. For example, either an MZI filter with 50-GHz FSR or one with 100-GHz FSR can be used as a duobinary mode splitting filter to extract USB and LSB duobinary modes. This configuration has the following merits:

- NRZ baseband signal processing only;
- broadband analog processing in optical carrier frequency;
- simple DWDM transmitter configuration.

The proposed configuration enables all baseband signal processing to be performed on binary NRZ signals and eliminates the complicated baseband analog processing needed to generate the three-level electrical signal required in the conventional DCS-RZ transmitter [6], [7]. Moreover, it allows us to relax the linearity requirement for the modulator drivers in ultra-high-speed DCS-RZ transmitters. Since all high-speed analog signal processing is conducted at the optical carrier frequency, this configuration is suitable for DWDM transmitters with ultrahigh-speed channels. Simultaneous DCS-RZ modulation by a single Mach-Zehnder interferometer (MZI) filter simplifies the DWDM transmitter configuration dramatically, when considering capacities in excess of terabits per second.

#### C. DCS-RZ Transmission System Using Duobinary-Mode Splitting of CS-RZ DPSK

The PSK/ASK conversion process described in Section II-B can also be applied to a DPSK signal where the phase and amplitude of the DPSK signal are modulated with a two-mode beat

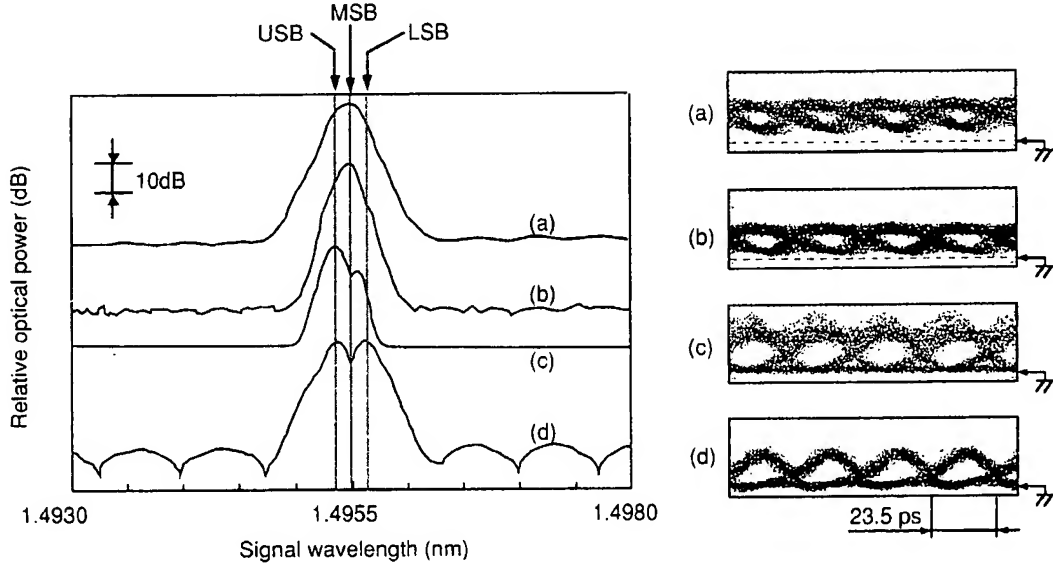


Fig. 7. Experimental verification of duobinary-mode splitting of 43 Gb/s DPSK signal for DCS-RZ signal generation. (a) Modulation spectra and directly-detected waveform of DPSK signal. (b) Modulation spectra and waveform MSB duobinary mode. (c) Modulation spectra and waveform USB duobinary mode. (d) Modulation spectra and waveform of DCS-RZ signal consisting of USB duobinary mode and LSB duobinary mode.

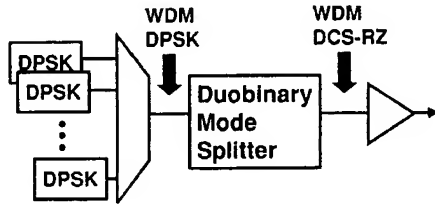


Fig. 8. DWDM upgrade of proposed DCS-RZ modulation scheme.

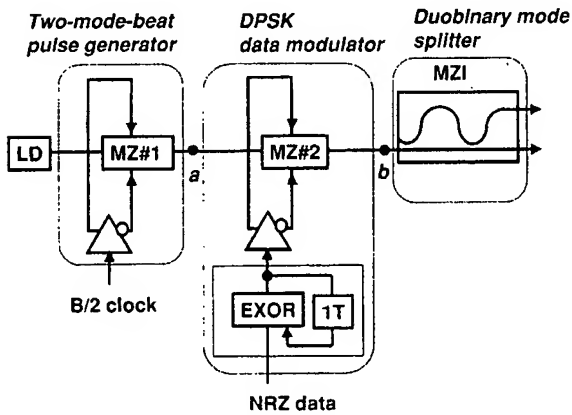


Fig. 9. Novel configuration of DCS-RZ transmitter using duobinary-mode splitting of CS-RZ DPSK signal.

pulse. Fig. 9 shows another novel DCS-RZ transmitter configuration. The only difference from Fig. 5 is that a two-mode beat pulser is used between the laser diode (LD) and the DPSK data modulator. Figs. 9 and 10 show the operation of the proposed transmitter. Since the two-mode beat pulse that is synchronized with input NRZ data is generated at point *a* in Fig. 9. The pulse spectrum is given in formula (1). The two-mode beat pulse shown in Fig. 10(a) is modulated by the DPSK signal. The

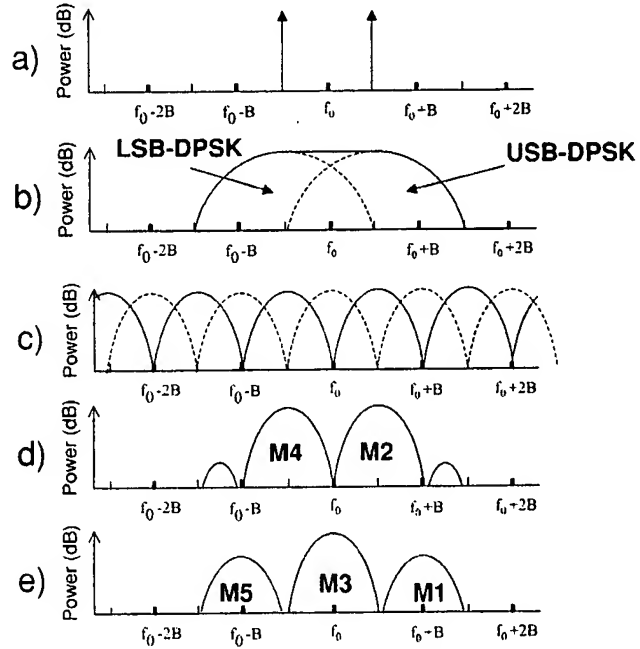


Fig. 10. Proposed DCS-RZ/CS-RZ DPSK signal modulation. (a) Spectra from two-mode beat pulse. (b) Modulation spectra of CS-RZ DPSK signal. (c) Transmission characteristic of duobinary-mode-splitting filter. (d) Spectral structure of DCS-RZ signal split from CS-RZ DPSK signal. (e) Spectral structure of Duobinary-RZ signal split from CS-RZ DPSK signal.

power spectrum of DPSK [1] for rectangular data pulse shape is given by

$$P_{\text{DPSK}}(\omega) = T \sin^2((\omega - \omega_c)T/2) / ((\omega - \omega_c)T/2)^2. \quad (7)$$

A twin DPSK signal spectrum separated by the line rate frequency shown in Fig. 10(b) is created at point *b* in Fig. 10. Here, we called this signal the “CS-RZ DPSK” signal. The power

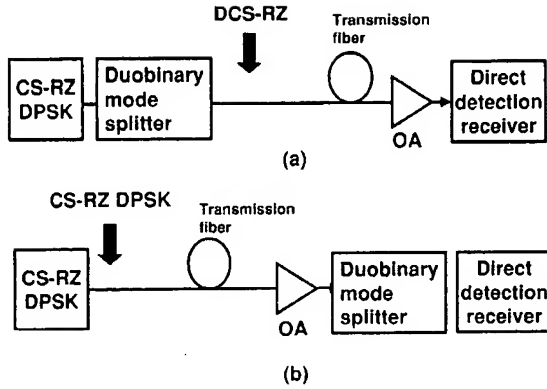


Fig. 11. System configuration using DCS-RZ format and CS-RZ DPSK format based on duobinary-mode splitting. (a) The single-channel system with the DCS-RZ transmission format. (b) The single-channel system with the CS-RZ DPSK transmission format.

spectrum of the CS-RZ DPSK is given in formula (8) using (7), as follows:

$$P_{\text{CS-RZ DPSK}}(\omega) = 2\omega_b^2 \cos^2((\omega - \omega_c)T/2) / ((\omega - \omega_c)^2 - (\omega_b/2)^2)^2. \quad (8)$$

Note that the directly detected waveform of the CS-RZ DPSK format is a sinusoidally modulated waveform with a frequency equal to the line rate. The pulsewidth of the intensity modulation is completely independent of the input data pattern, which is desirable to enhance the nonlinearity tolerance. The CS-RZ DPSK signal contains two DPSK modes [upper-side-band (USB)-DPSK and lower-side-band (LSB)-DPSK], shown in Fig. 10(a), which are mode-locked to each other. Since each DPSK mode has three duobinary modes, as shown in Fig. 6, and the LSB-duobinary mode in USB-DPSK overlaps the USB-duobinary mode in LSB-DPSK, these two duobinary modes form a combined duobinary mode (M3). As a result, the CS-RZ DPSK signal has five duobinary modes: USB-duobinary mode (M1) and MSB-duobinary mode (M2) in USB-DPSK; combined duobinary mode (M3); MSB-duobinary-mode (M4); and LSB-duobinary mode (M5), as shown in Fig. 10. The odd duobinary modes of M1, M3, and M5 of the CS-RZ DPSK signal transmit the same digital data signal, but have the opposite logic to the even modes of M2 and M4. Using an MZI filter with an FSR equal to the line rate, the odd and even modes of CS-RZ DPSK can be split to form two separate RZ signals—a duobinary RZ signal and a DCS-RZ signal, as shown in Fig. 10(d) and (e).

Compared with the scheme described in Section II-B, the loss in the duobinary-mode-splitting MZI filter in this configuration is reduced, because the scheme described in Section II-B uses the rejection band of an MZI filter, while the scheme described in this section uses the passband of an MZI filter. The pulsewidth of the DCS-RZ becomes more uniform through the use of the two-mode beat pulse, so it is possible to generate a DCS-RZ signal from a CS-RZ DPSK signal with higher nonlinearity tolerance compared with that described in Section II-B.

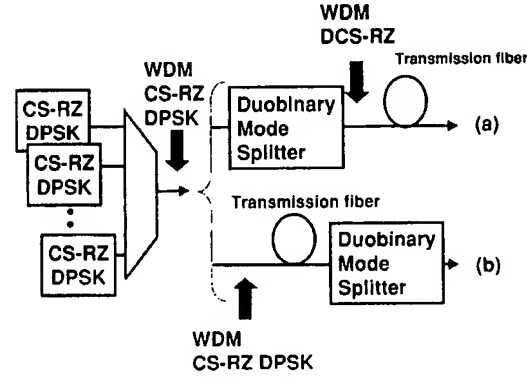


Fig. 12. DWDM upgrade of duobinary-mode splitting in proposed RZ system. (a) The DWDM system configuration with DCS-RZ transmission format. (b) The DWDM system configuration with CS-RZ DPSK transmission format.

#### D. CS-RZ DPSK Transmission System Using Duobinary-Mode Splitting

In the previous section, the transmission format in the transmission fiber is DCS-RZ, and the CS-RZ DPSK format is just used as the signal in the DCS-RZ transmitter, as shown in Fig. 11(a), where OA is the optical preamplifier. Namely, the intensity modulation is used for data transmission, and phase modulation is only used for reducing the bandwidth of the intensity-modulated RZ signal. When the duobinary-mode-splitting PSK/ASK process is conducted in the receiver, it is possible to use a CS-RZ DPSK signal as the transmission format. In this section, we consider the CS-RZ DPSK format as a transmission format in the transmission fiber, as shown in Fig. 11(b). In this case, optical phase modulation is used for data transmission. The periodic intensity modulation and alternate phase modulation added in the two-mode beat-pulse generation section are used for enhancing the transmission performance. When the fiber nonlinearity is negligible at small channel power, both system configurations shown in Fig. 11(a) and (b) offer the same transmission performance. If the transmission system is strongly affected by fiber nonlinearity, different transmission performance between these system configurations is expected.

The transmitter configuration of CS-RZ DPSK is the same as that of DCS-RZ shown in Fig. 9, except for the duobinary-mode-splitting MZI filter. The modulation bandwidth of CS-RZ DPSK format is  $3B$ , as shown in Fig. 10(b), which is comparable to that of the CS-RZ format shown in Fig. 2(b). Therefore, the CS-RZ DPSK signal offers a significant bandwidth reduction. Its bandwidth is also smaller than those of the RZ and RZ DPSK [15] formats. Since the directly detected waveform is sinusoidal, the pulsewidth is constant and does not depend on the input data pattern. This feature is attractive to enhance the fiber nonlinearity tolerance. In the receiver of the CS-RZ DPSK system, the transmitted CS-RZ DPSK signal is converted to intensity-modulated signals—the DCS-RZ format shown in Fig. 10(d) or the duobinary RZ format shown in Fig. 10(e), using the MZI filter as the duobinary-mode splitter. It should be noted that it is very interesting to realize large dispersion tolerance in the receiver while keeping the nonlinear-tolerant RZ transmission characteristics, when the converted duobinary RZ

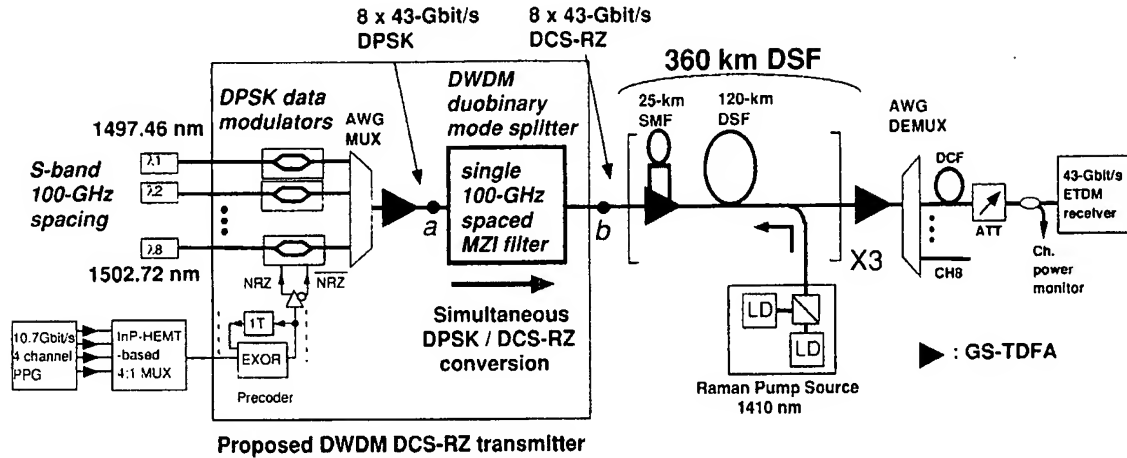


Fig. 13. Experimental setup of DWDM DCS-RZ transmission using duobinary-mode splitting of the DPSK signal.

signal shown in Fig. 10(e) is further filtered to yield the single duobinary mode M3. This mode-splitting operation from the CS-RZ DPSK to single duobinary mode M3 signal can be easily performed by using only a bandpass filter, as is confirmed in Section IV.

Similarly, the attractive WDM upgrade of the configuration is possible, as shown in Fig. 12. It is also possible to convert the WDM CS-RZ DPSK signals into WDM DCS-RZ signals by a single MZI filter, both in the transmitter and the receiver, when the FSR of the MZI filter is equal to the WDM spacing. When the duobinary-mode splitting is conducted in the transmitter [see Fig. 12(a)], the transmission format is DCS-RZ and the digital data is transferred by intensity modulation. When the duobinary-mode splitting is conducted in the receiver [see Fig. 12(b)], the transmission format is CS-RZ DPSK and the data is transferred by PSK modulation. The next section introduces experiments that verify the proposed configurations.

### III. EXPERIMENTAL RESULTS

#### A. $8 \times 43$ -Gb/s DWDM DCS-RZ Signal Transmission Using Duobinary-Mode Splitting

Fig. 13 shows the proposed DWDM DCS-RZ transmission system using the duobinary-mode splitting of the DPSK signal described in Section II-B. The DWDM transmitter consists of a push-pull-type Mach-Zehnder (MZ) modulator as a DPSK data modulator [10] for each channel and a single 100-GHz-spaced MZI periodic optical filter, whose rejection-band center frequency was tuned to the 100-GHz-spaced optical carrier frequencies in the *S* band.

In the DPSK data modulator, a 42.7-Gb/s NRZ complementary pseudorandom binary sequence (PRBS) signal with a pattern length of  $2^7 - 1$  was generated by a 4:1 MUX using an InP HEMT multiplexer integrated circuit (IC) [11]. The precoder circuit, consisting of a 1-b delay and an exclusive OR (EXOR) circuit indicated within the dotted square in Fig. 13, was omitted from the experimental system, because the test signal was a PRBS pattern. The push-pull-type MZ modulator [12], biased at the transmission null point, was modulated by the 42.7-Gb/s complementary NRZ PRBS signals that are corresponding to

the binary precoded NRZ signal at point *b* in Fig. 5. Since the driving signals are NRZ, the driver amplifiers (not indicated in Fig. 13) do not have strict linearity requirements, unlike the case of the conventional DCS-RZ transmitter [6], [7]. Fig. 14 shows the conversion process. Eight 100-GHz-spaced optical carrier signals, whose wavelengths ranged from 1497.46 nm (channel 1) to 1502.72 nm (channel 8), were simultaneously modulated into  $8 \times 42.7$ -Gb/s DWDM DPSK signals. Fig. 14(a) shows the WDM spectra measured at point *a* in Fig. 13. The 100-GHz-spaced rejection band center frequency of the MZI filter was tuned to coincide with the 100-GHz-spaced optical carrier frequency, as shown in Fig. 14(b). Since the MZI filter acts as a WDM duobinary-mode-splitting filter with a PSK/ASK-conversion function under this frequency allocation, as described in Section II-B, the  $8 \times 42.7$ -Gb/s DWDM DPSK signals were simultaneously converted into DWDM DCS-RZ signals [shown in Fig. 14(c)]. This configuration does not require any synchronization mechanism between data modulator and pulse generator in the conventional DCS-RZ transmitter. The detected waveform shown in Fig. 12(c) confirms that the converted signal was an RZ-shaped signal with a clear eye opening.

The DWDM DCS-RZ signals were boosted up to the channel power of +5 dBm by using a gain-shifted Tm-doped fluoride amplifier (GS-TDFA) postamplifier [13]. The dispersion-managed 360-km transmission line consisted of three 120-km DSF spans. Each span consisted of a 120-km DSF with distributed Raman amplification and a GS-TDFA in-line repeater [13]. The GS-TDFA in-line repeater used in this experiment employed the two-stage configuration with a single-pass first stage and a double-pass second stage. The GS-TDFAs utilized an intermediate 25-km single-mode fiber (SMF) for dispersion compensation, in addition to the two-stage configuration, and achieved low-noise figures (less than approximately 5.8 dB) and high pumping efficiency of up to approximately 42% in the signal wavelength region.

Distributed Raman amplification in the *S* band [14] was realized using three polarization-multiplexed LD pump light sources. The pump wavelength was 1410 nm, and the signal wavelength experiencing the highest Raman gain was approximately 1505 nm. The ON-OFF Raman gain at 1500 nm



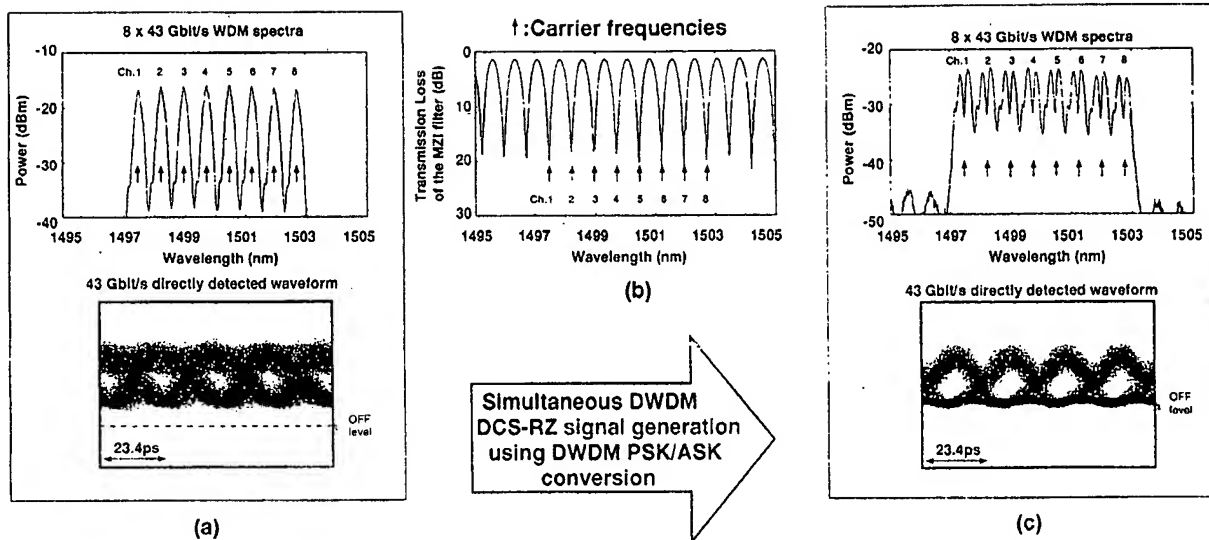


Fig. 14. Simultaneous DWDM DCS-RZ generation using wideband PSK/ASK conversion. (a) DWDM DPSK signals at the input of the 100-GHz-MZI filter. (b) Frequency allocation of MZI filter and optical carriers. (c) Converted DWDM DCS-RZ signals.

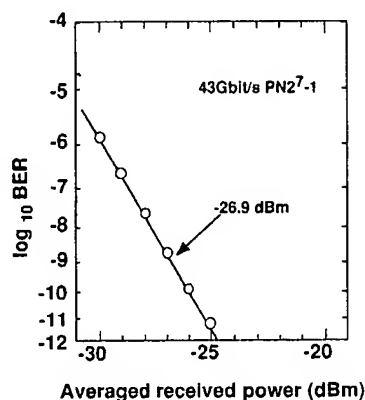


Fig. 15. Back-to-back performance of proposed DCS-RZ modulation scheme.

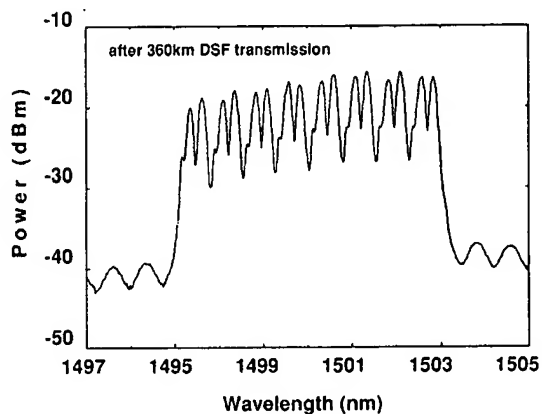


Fig. 16. WDM spectra after 360-km DSF transmission.

was set at 15 dB in order to maximize the improvement in the signal-to-noise ratio with the pump power launched into the DSF of approximately 300 mW. The average span loss and local dispersion of the three sections were 30 dB and  $-3.6$  ps/nm/km, respectively, at the wavelength of 1500 nm. In the receiver, transmitted signals were wavelength-division multiplexed/demultiplexed by a flat-top arrayed-waveguide grating (AWG) filter. Dispersion compensation in the receiver set the total link dispersion to zero at the signal wavelengths. The 42.7-Gb/s DCS-RZ signals were directly detected and electrically demultiplexed to check the bit error rate (BER). The receiver configuration is the same as that in [6].

Fig. 15 shows the back-to-back BER performance in the 100-GHz-spaced WDM configuration for channel 4. There is no error floor and the high sensitivity of  $-26.9$  dBm was obtained at the BER of  $10^{-9}$ . This result shows that the RZ code offers the same coding rule as the DCS-RZ format with small initial ISI. Fig. 16 shows the WDM spectra after 360-km DSF transmission. Four-wave mixing was effectively suppressed in

the 100-GHz-spaced DWDM transmission because of the large local dispersion of the DSF in the *S* band. Good eye opening was obtained after transmission at channel 4, as shown in Fig. 17.

BER measurements after the 360-km DSF transmission were conducted by testing all 10.7-Gb/s tributary channels after 1:4 demultiplexing by InP-HEMT-IC-based demultiplexer ICs. All 42.7-Gb/s channels were successfully transmitted over the 360-km DSF transmission line with *Q* factors higher than 15 dB. Using FEC, error-free (i.e., bit error rates better than  $10^{-50}$ ) transmission is expected over the typical system life, as shown in Fig. 17. The regenerative repeater spacing of 360 km was demonstrated in an *S*-band 100-GHz-spaced 42.7-Gb/s/channel DWDM transmission using a DSF-based dispersion management line for the first time. These results show that the proposed DCS-RZ transmitter using duobinary-mode splitting is desirable for DWDM systems that offer ultrahigh-speed channels; it achieves both high signal spectral efficiency, over 0.4 b/s/Hz, and an extremely simple DWDM transmitter configuration.

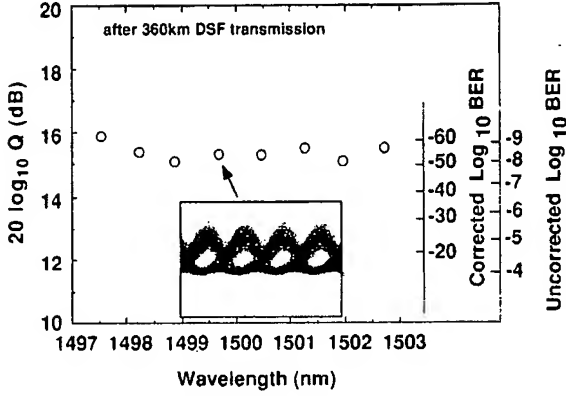


Fig. 17. Eight-channel WDM transmission performance after 360 km.

### B. 43-Gb/s CS-RZ-DPSK Signal Transmission Using Duobinary-Mode Splitting

Fig. 18 shows the experimental setup confirming the duobinary-mode-splitting scheme in the CS-RZ DPSK signal transmission described in Section II-D. The proposed transmitter consists of a DPSK data modulator [10] and a two-mode beat-pulse generator using two-stage push-pull MZ modulators. In the DPSK data modulator, baseband NRZ complementary signals were generated by an InP-HEMT-multiplexer IC [11] through the input of a 42.7-Gb/s PRBS signal with the pattern length of  $2^7 - 1$ . A precoder consisting of a 1-b delay and an exclusive OR circuit was omitted in the experimental system, because the test signal was a 42.7-Gb/s PRBS pattern. The complementary PRBS NRZ signals are amplified to drive the first MZ modulator (MZ#1) biased at the transmission null point. An optical carrier signal at the wavelength of 1552.52 nm was modulated to yield a 42.7-Gb/s DPSK signal by the first MZ modulator.

The second MZ modulator (MZ#2) biased at the transmission null point was used as an RZ pulse generator that modulates the optical phase of the DPSK signal alternately with  $\pi$  phase flip. Since the order of the two MZ modulators can be exchanged due to the linear system, the transmitter configuration is the same as that shown in Fig. 9, except for the MZI filter. Therefore, the output RZ signal obtained from MZ#2 was a CS-RZ DPSK signal [9]. Since the CS-RZ DPSK uses optical phase modulation for data transmission, the directly detected waveform is a 42.7-GHz sinusoidal clock signal with a CS narrow-bandwidth signal spectrum, as shown in Fig. 19(a). The optical modulation bandwidth measured at  $-20$  dB down was 86 GHz. The dispersion compensation fiber (DCF) of  $-120$  ps/nm was used in the transmitter for prechirping. The transmission fiber consisted of two spans of 100-km DSF, having dispersion and a dispersion slope of  $+1.7$  ps/nm/km and  $+0.065$  ps/km/nm<sup>2</sup>, respectively, at 1552.52 nm. In the receiver, the transmitted CS-RZ DPSK signal was amplified and fed to a PSK-ASK conversion filter. Two types of conversion filters were tested. One was a polarization-independent MZI filter with a free spectral range of 50 GHz; the other is a bandpass filter with a full-width at half-maximum (FWHM) of 33 GHz. The DCF ( $-240$  ps/nm) in the receiver was set so as to keep total dispersion (including

the DCFs) to 0 ps/nm. The passband center of these filters was tuned to coincide with the optical carrier frequency. Since these filters act as optical duobinary filters with this band allocation, the CS-RZ DPSK signals are converted into duobinary signals [the M3 component shown in Fig. 10(e) and described in Section II-C]. The measured waveform and spectrum converted by the bandpass filter are shown in Fig. 19(b). The measured  $-20$ -dB down bandwidth of the converted duobinary signal was reduced to 68 GHz. The receiver was a conventional single-end direct-detection receiver. The back-to-back receiver sensitivities of the CS-RZ and the CS-RZ DPSK were  $-27.6$  dBm and  $-27.2$  dBm (with the 50-GHz MZI filter)/ $-20.9$  dBm (with the bandpass filter), respectively, at a BER of  $10^{-9}$ . Since the proposed configuration enables simple baseband signal data processing of just binary NRZ signals, this configuration is suitable for ultrahigh-speed channel modulation and detection.

Figs. 20 and 21 show the dispersion tolerance and power tolerance characteristic of the CS-RZ DPSK format, respectively. As shown in Fig. 20, the dispersion tolerance of the conventional CS-RZ (the white squares) is only 50 ps/nm. On the other hand, the CS-RZ DPSK offers greatly enhanced dispersion tolerance, up to 80 ps/nm (the black circles) with the 50-GHz MZI filter and up to 190 ps/nm with the bandpass filter (the white circles). Since the CS-RZ DPSK signal has a flat signal spectrum in the vicinity of the carrier frequency, as shown in Fig. 19(a), it is easy to extract the duobinary-mode spectrum using conventional optical filters. We compared the CS-RZ DPSK and CS-RZ in terms of their nonlinearity tolerance by measuring the dynamic range of repeater output, i.e., the channel powers yielding  $Q$  factors higher than 15.6 dB, as shown in Fig. 21. The dynamic ranges are 13.2 dB (from  $-3.2$  dBm to  $+10.0$  dBm) for CS-RZ and 13.4 dB (from  $-2.2$  dBm to  $+11.2$  dBm) for CS-RZ DPSK. The CS-RZ DPSK has 1.2 dB higher power tolerance than does the CS-RZ. The lower limit is 1 dB larger than that of the CS-RZ, because of the use of the single-end receiver and the insufficient driving voltage of the DPSK data modulation section. The DPSK signal inherently offers 3 dB higher sensitivity than intensity modulation when using a balanced receiver [10]. Because a single-end receiver was used in this experiment, the lower limit of the CS-RZ DPSK in this experiment should be the same as that of the CS-RZ. This confirms that the proposed CS-RZ DPSK has superior SPM tolerance and larger dispersion tolerance than the CS-RZ using duobinary-mode splitting.

## IV. DISCUSSION

In the literature [15], the RZ-DPSK was shown to have superior transmission performance in terms of XPM tolerance, compared with the conventional RZ format. We conducted simulations to compare the 100-GHz-spaced four-channel WDM performance of the CS-RZ DPSK with that of DCS-RZ in terms of XPM impairment. Fig. 22(a) and (b) shows the system configuration for the DCS-RZ and CS-RZ DPSK, respectively. In Fig. 22(a), a simultaneous duobinary-mode-splitting filter is implemented in the transmitter to generate DWDM DCS-RZ signals. In Fig. 22(b), a mode-splitting filter is implemented in the receiver to demodulate the CS-RZ DPSK signal. The tested link

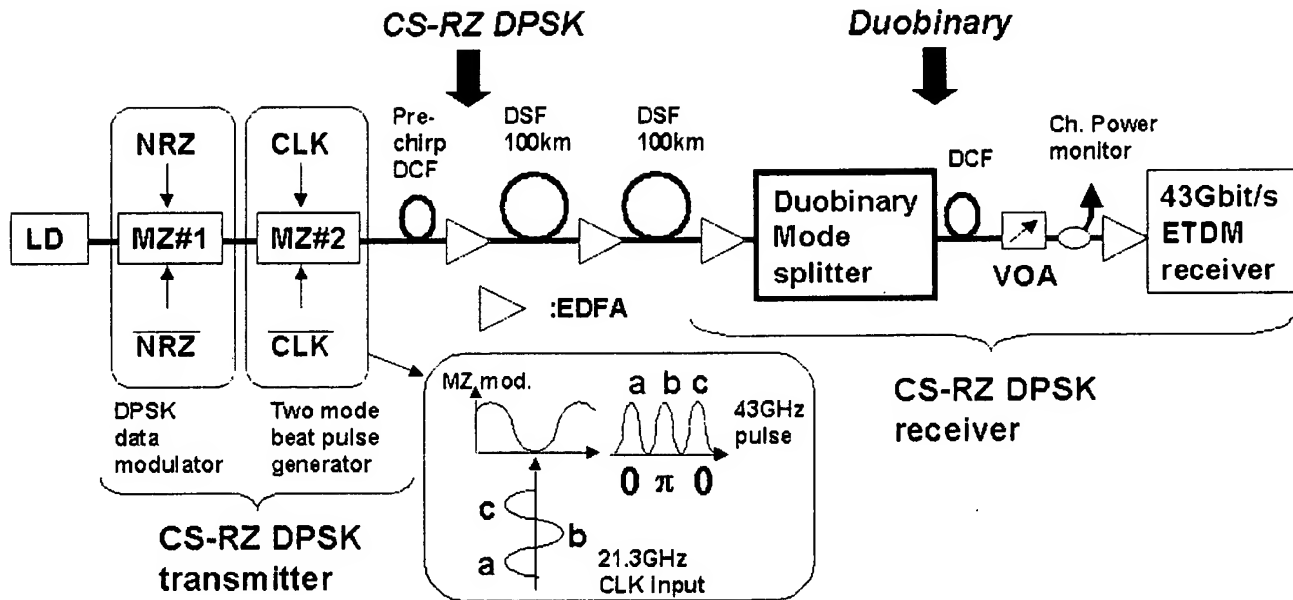


Fig. 18. Experimental setup of CS-RZ DPSK transmission using duobinary-mode splitting in the detection process.

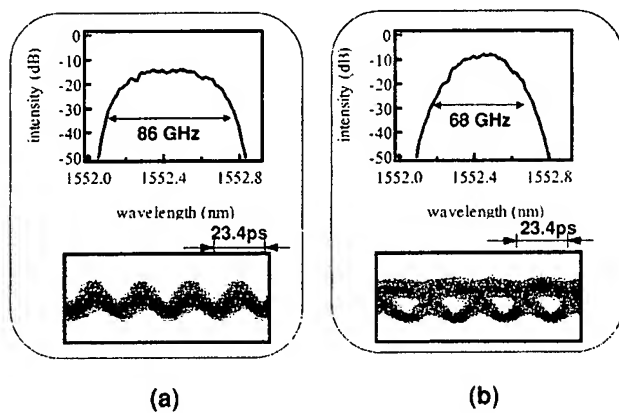


Fig. 19. Signal spectra and waveforms in 43-Gb/s duobinary-mode-splitting process of the CS-RZ DPSK signal. (a) CS-RZ DPSK. (b) Duobinary after the PSK/ASK duobinary-mode-splitting conversion filter.

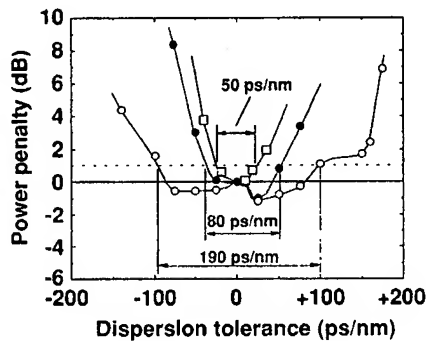


Fig. 20. Enlargement of dispersion tolerance by duobinary-mode splitting of the 43-Gb/s CS-RZ DPSK signal.

consists of two spans of 100-km DSF and an inline optical amplifier repeater. The local dispersion and the loss in signal wave-

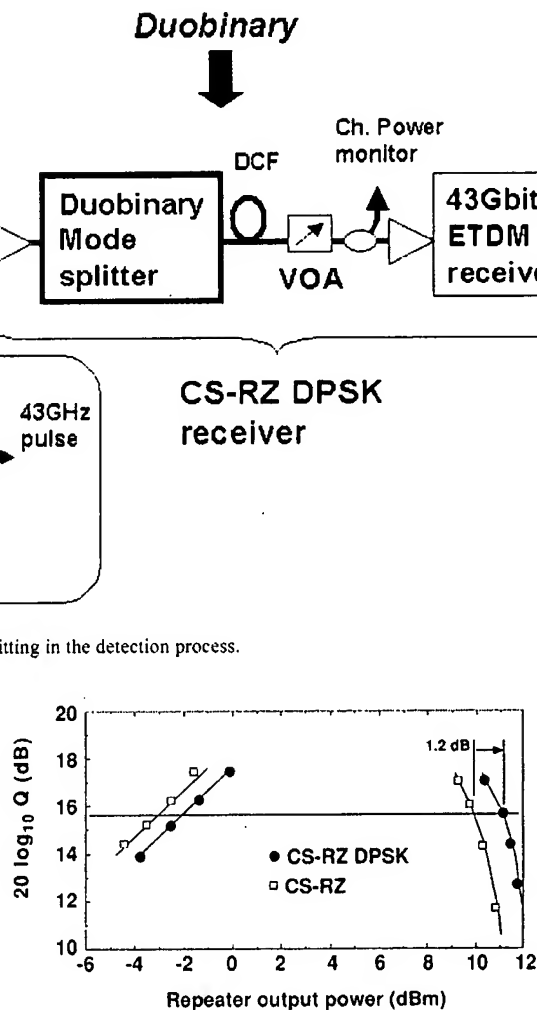


Fig. 21. Enhancement of SPM tolerance by the CS-RZ DPSK signal transmission.

length were +2.0 ps/nm and 0.2 dB/km, respectively, and the XPM impairment dominated. The line rate was set to 43 Gb/s. The dispersion management scheme was inline dispersion management conducted in the  $L$  band. The mode-splitting filter is an MZI filter with an FSR of 50 GHz. The channel rate was set to 43 Gb/s. Fig. 23 shows that the DCS-RZ format offers almost the same dispersion tolerance as the CS-RZ DPSK at channel powers of less than 2 dBm (linear transmission case). Since the system performance is linear, the dispersion tolerance performance is not dependent on the location of the mode-splitting filter. For channel powers of more than +4 dBm, however, the power tolerance of the DCS-RZ signal in the center channel is severely limited. This is due to XPM impairment. The CS-RZ DPSK signal, on the other hand, offers enhanced power tolerance—3 dB higher than the DCS-RZ. This result shows that the CS-RZ DPSK also has superior XPM tolerance in the DWDM based on 43-Gb/s channels. These attractive results were expected, since the CS-RZ DPSK has the same features as the RZ DPSK [15]: since its amplitude waveform is sinusoidal, which is PSK-modulated, the XPM-induced nonlinear phase shift in each WDM channel is less dependent on the data pattern as compared

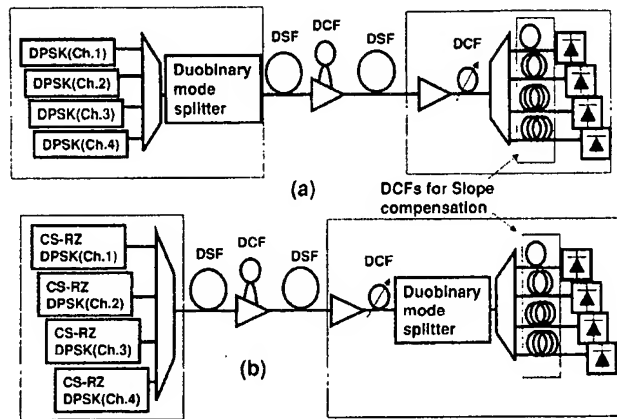


Fig. 22. Performance comparison of CS-RZ DPSK and DCS-RZ using duobinary-mode splitting with regard to XPM impairment.

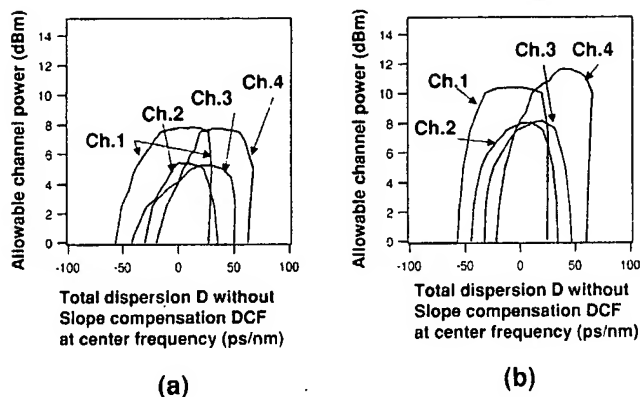


Fig. 23. Eye opening map of CS-RZ DPSK and DCS-RZ signal transmission. (a) DCS-RZ. (b) CS-RZ DPSK.

with intensity-modulated RZ. Therefore, the PSK/ASK conversion process cancels the nonlinear phase shifts in two adjacent bits induced by the XPM. In addition, the modulation bandwidth of the CS-RZ DPSK is more compact than that of conventional RZ DPSK [15]. Therefore, the CS-RZ DPSK has excellent DWDM performance when XPM impairment is dominant.

## V. CONCLUSION

This paper proposed bandwidth-reduced RZ modulation formats that use a novel duobinary-mode-splitting scheme in wide-band PSK/ASK conversion for the modulation and detection processes for DCS-RZ. The CS-RZ DPSK was also proposed as a novel transmission format and places the duobinary-mode-splitting scheme in the receiver. These novel RZ formats were shown to be very suitable for realizing DWDM transport systems based on high-speed channels of more than 40 Gb/s with spectrum efficiencies higher than 0.4 b/s/Hz. We experimentally demonstrated that the proposed modulation and detection scheme greatly simplifies the DWDM transmitter and receiver configuration, if the FSR of the PSK/ASK conversion filter is equal to the WDM channel spacing. Large tolerance against several fiber nonlinearities and wide dispersion tolerance characteristics were confirmed by testing the proposed CS-RZ DPSK

format in DSFs at the channel rate of 43 Gb/s. These novel RZ formats were shown to be desirable to enhance the performance of DWDM transmission systems based on ultrahigh-speed channels.

## ACKNOWLEDGMENT

The authors would like to thank M. Kawachi, K.-I. Sato, K. Hagimoto, and H. Toba for their continuous encouragement; H. Toba, M. Muraguchi, E. Sano, T. Enoki, T. Otsuji, Y. Yamane, K. Murata, and M. Yoneyama for their ongoing support with regard to InP HEMT ICs and several fruitful discussions; T. Ishibashi, H. Ito, and N. Shimizu for an illuminating discussion on uni-traveling-carrier photodiodes (UTC-PDs); K. Noguchi and H. Miyazawa for useful discussions on the ultrahigh-speed MZ modulator; M. Shimizu, H. Masuda, and S. Aozasa for their support and their useful discussions with regard to S-band hybrid GS-TDFA/Raman amplifiers; and K. Yonenaga and Y. Inoue for their valuable discussion throughout this work.

## REFERENCES

- [1] K. Yonenaga and S. Kuwano, "Dispersion-tolerant optical transmission system using duobinary transmitter and binary receiver," *J. Lightwave Technol.*, vol. 15, pp. 1530–1537, Aug. 1997.
- [2] A. Matsuura, Y. Kazushige, Y. Miyamoto, and H. Toba, "High-speed transmission system based on optical modified duobinary signals," *Electron. Lett.*, vol. 35, pp. 736–737, 1999.
- [3] Y. Miyamoto, K. Yonenaga, A. Hirano, and M. Tomizawa, "X × 40-Gbit/s DWDM transport system using novel return-to-zero formats with modulation bandwidth reduction," *IEICE Trans. Commun.*, vol. E85-B, pp. 374–385, 2002.
- [4] Y. Miyamoto, A. Hirano, K. Yonenaga, A. Sano, H. Toba, K. Murata, and O. Mitomi, "320 Gbit/s (8 × 40Gbit/s) WDM transmission over 367 km with 120 km repeater spacing using carrier-suppressed return-to-zero format," *Electron. Lett.*, vol. 35, pp. 2041–2042, 1999.
- [5] A. Hirano, M. Asobe, K. Sato, K. Yonenaga, Y. Miyamoto, H. Takara, I. Shake, H. Miyazawa, and M. Abe, "Dispersion tolerant 80 Gbit/s optical-time-division-multiplexing using a duty- and phase-control technique," in *Tech. Dig. of ECOC'99*, Nice, France, 1999, pp. 2–36.
- [6] Y. Miyamoto, K. Yonenaga, A. Hirano, H. Toba, K. Murata, and H. Miyazawa, "100 GHz-spaced 8 × 43Gbit/s DWDM unrepeated transmission over 163 km using duobinary-carrier-suppressed return-to-zero format," *Electron. Lett.*, vol. 37, pp. 1395–1396, 2001.
- [7] Y. Miyamoto, K. Yonenaga, and S. Kuwahara, "Dispersion-tolerant RZ signal transmission using baseband differential code and carrier-suppressed modulation," in *Tech. Dig. ECOC'98*, Madrid, Spain, 1998, pp. 351–352.
- [8] Y. Miyamoto, A. Hirano, S. Kuwahara, Y. Tada, H. Masuda, S. Aozasa, K. Murata, and H. Miyazawa, "S-band 3 × 120km DSF transmission of 8 × 42.7-Gbit/s DWDM duobinary-carrier-suppressed RZ signals generated by novel wideband PM/AM conversion," in *Tech. Dig. OAA2001*, Stresa, Italy, 2001, Paper PD6.
- [9] Y. Miyamoto, A. Hirano, S. Kuwahara, Y. Tada, K. Murata, and H. Miyazawa, "Carrier-suppressed differential phase shift keying format for ultra-high-speed channel transmission," presented at the OAA2002, Vancouver, Canada, submitted in Feb. 2002, Paper OTuB2.
- [10] K. Yonenaga, S. Aizawa, N. Takachio, and K. Iwashita, "Reduction of four-wave mixing induced penalty in unequally spaced WDM transmission system by using optical DPSK," *Electron. Lett.*, vol. 32, pp. 2118–2119, 1996.
- [11] T. Otsuji, E. Sano, Y. Imai, and T. Enoki, "40-Gbit/s IC's for future light-wave communications systems," in *Tech. Dig. GaAs-IC Simp.*, 1996, pp. 14–17.
- [12] K. Noguchi, H. Miyazawa, and O. Mitomi, "LiNbO<sub>3</sub> high-speed modulators," in *Tech. Dig. CLEO*, Pacific Rim, 1999, Paper FS2, pp. 1267–1268.

- [13] S. Aozasa, H. Masuda, H. Ono, T. Sakamoto, S. Kanamori, Y. Ohishi, and M. Shimizu, "1480-1510 nm-band Tm doped fiber amplifier (TDFA) with a high power conversion efficiency of 42%," in *Tech. Dig. OFC2001*, Anaheim, CA, 2001, Paper PD1.
- [14] H. Masuda and S. Kawai, "Ultra wide-band Raman amplification with a total gain-bandwidth of 132 nm of two gain-bands around 1.5  $\mu$ m," in *Tech. Dig. of ECOC '99*, Nice, France, 1999, pp. 2-146.
- [15] T. Miyano, M. Fukutoku, K. Hattori, and H. Ono, "Suppression of degradation induced by SPM/XPM+GVD in WDM transmission using bit-synchronous intensity modulated DPSK signal," in *Tech. Dig. OECC2000*, Makuhari, Japan, Paper 14D3-3.

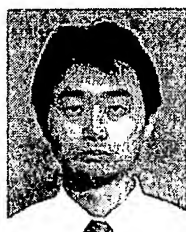


**Yutaka Miyamoto** (M'93) was born in Tokyo, Japan, on December 8, 1963. He received the B.E. and M.E. degrees in electrical engineering from Waseda University, Tokyo, Japan, in 1986 and 1988, respectively.

In 1988, he joined NTT Transmission Systems Laboratories, Yokosuka, Kanagawa, Japan, where he engaged in research and development on high-speed optical communications systems, including the 10-Gb/s terrestrial optical transmission system called the FA-10G system. Currently, he is a Senior Research Engineer and Supervisor at NTT Network

Innovation Laboratories. His current research interest includes high-capacity systems using ultrahigh-speed channels and their related devices.

Mr. Miyamoto is a Member of the Institute of Electronics, Information, and Communication Engineers (IEICE) of Japan. He received the Best Paper Award of the first Optoelectronics and Communication Conference (OECC'96) in 1996 from the IEICE.



**Akira Hirano** was born in Hyogo Prefecture, Japan, on November 4, 1967. He received the B.S. degree in physical chemistry and the M.S. degree in astrophysics from Osaka University, Osaka, Japan, in 1990 and 1993, respectively.

In 1993, he joined Nippon Telegraph and Telephone Corporation (NTT), working in the lightwave communications area. His main interests are in high-speed lightwave transport systems, optical signal processing, and ultrashort-pulse generation.

Mr. Hirano is a Member of the Institute of Electronics, Information, and Communication Engineers (IEICE) of Japan.



**Shoichiro Kuwahara** was born in Yamaguchi, Japan, on October 31, 1970. He received the B.S. and M.S. degrees in electrical engineering from Shizuoka University, Hamamatsu, Japan, in 1993 and 1995, respectively.

In 1995, he joined the NTT Optical Network Systems Laboratories, Yokosuka, Japan, where he was engaged in the research and development of dispersion equalization schemes for installing and operating high-speed optical transmission systems.

His current research interests include high-speed communication systems and related devices for 40-Gb/s channels.

Mr. Kuwahara is a Member of the Institute of Electronics, Information, and Communication Engineers (IEICE) of Japan.

**Masahito Tomizawa** (M'95) received the B.E. degree in applied physics, the M.Sc. degree in physics, and the Dr. Eng. degree in applied physics from Waseda University, Tokyo, Japan, in 1990 and 1992, and 2000, respectively.

In 1992, he joined NTT Transmission Systems Labs, where he was engaged in research and development of high-speed optical ring architecture, forward error correcting codes in fiber-optic systems, and automatic dispersion equalization. He then joined NTT Network Service Systems Labs, where he devoted himself to the installation of 10-Gb/s ring systems in all of NTT's network. Since 1999, he has been with NTT Network Innovation Labs, where his main job is international standardization of fiber-optic systems in International Telecommunication Union-Telecommunication (ITU-T). He is also engaged in research and development of 40-Gb/s systems.

Dr. Tomizawa is a Member of the Institute of Electronics, Information, and Communication Engineers (IEICE) of Japan. He received the Young Engineer Award from the IEICE in 1998.

**Yasuhiro Tada** was born in Miyagi, Japan, on January 19, 1957. He received the M.S. degree from Tohoku University, Sendai, Japan, in 1982.

In 1982, he joined NTT Yokosuka Electrical Communications Laboratories, Yokosuka, Kanagawa, Japan, where he was engaged in research and development of digital speech signal processing (bit rate reduction CODEC) and optical cross-connect switching technologies. From 1998 to 2000, he was active in the development of upgradable submarine WDM transmission commercial system. Since 2000, he has been Group Leader of the High-Speed Lightwave Transport System Research Group, NTT Network Innovation Laboratories, Yokosuka, Japan, heading research on high-speed lightwave communication technologies.

Mr. Tada is a Member of the Institute of Electronics Information and Communication Engineers (IEICE) of Japan.

# A NOVEL CHIRPED RETURN-TO-ZERO TRANSMITTER AND TRANSMISSION EXPERIMENTS

Fenghai Liu, Christophe Peucheret, Xueyan Zheng, Rune J.S. Pedersen and  
Palle Jeppesen

Research Center COM, Technical University of Denmark, Building 349, DK-2800 Lyngby, Denmark  
Phone: +45-45253845, Fax: +45-45936581, Email: lf@com.dtu.dk

*Abstract: A new 10 Gb/s chirped return-to-zero transmitter using CW light modulated by only one external modulator is proposed. Transmission over 3600 km of standard single mode fibre is performed in a re-circulating loop set-up with 80 km amplifier span.*

## Introduction

As the requirement for transmission of large capacity over long distance increases, different technologies to fulfill this purpose have been investigated. Among them, the return-to-zero (RZ) modulation format has become of great importance at high bit-rate, because of its robustness to fibre non-linearity and dispersion. Many of the transmission experiments achieving the longest distances with large capacity have used RZ format [1-3].

There are many different ways to obtain an optical RZ format, and in most cases data is converted into RZ format in the optical domain by externally modulating the signal onto an optical short pulse train with a fixed repetition rate. Such an optical short pulse train can be generated by sources like mode-locked lasers [4] or gain-switched DFB lasers [5]. A commonly used method referred to as chirped return-to-zero (CRZ) is obtained by modulating CW light in a chain of external modulators: first the amplitude of the light is modulated using the NRZ signal; second the amplitude is modulated again using a bit-synchronized clock to get the RZ pulse shape; last the phase is modulated using a bit-synchronized clock to add a chirp on the pulse. The signal generated in this way has shown very good performance in transmission over long distances [1,2].

In this paper, we propose a new and simplified way to generate the CRZ pulses using only one external modulator and a CW light source. Using such a CRZ transmitter, 10 Gb/s transmission over 3600 km of standard single mode fibre has been obtained in a re-circulating loop set-up with 80 km amplifier span. Power penalty at BER of  $10^{-9}$  is less than 6 dB after the transmission.

## Structure of the CRZ transmitter

The schematic diagram of the CRZ transmitter is shown in Fig. 1. An electrical 2:1 selector is used to generate 10 Gb/s RZ electrical pulses. A 10Gb/s NRZ signal (pattern =  $2^{31}-1$ ) is put into Data1 input of the selector while Data2 input is connected to a constant "space" which is the ground in this case. The Select-control is connected to a 10 GHz clock to select Data1 input at the rising edge of the clock and Data2 input at the falling edge. As a result, a 10 Gb/s RZ signal is obtained at Output of the selector. The eye-diagram of the electrical RZ pulses is shown in Fig. 2 (a). In principle, AND logic operation between a 10 Gb/s NRZ signal and a synchronized 10 GHz clock in an electrical gate can also generate 10 Gb/s RZ signal.

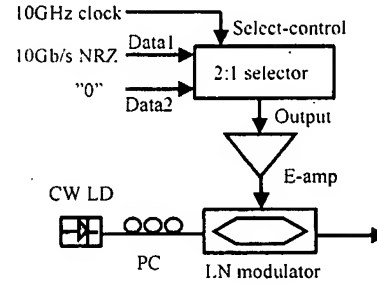


Figure 1: Schematic diagram of the CRZ transmitter

CW light from a DFB semiconductor laser is coupled into a Lithium Niobate (LN) Mach-Zehnder modulator via a polarization controller (PC). When the RZ signal generated from the 2:1 selector is amplified by an electrical amplifier (E-amp), and applied to one electrode of the LN modulator with a proper DC bias, a 10 Gb/s RZ optical signal is generated as shown in Fig. 2 (b). Since only one electrode of the LN modulator is used, a bit-synchronized chirp is automatically added to the RZ pulse. To show this, the electric field  $E$  after the modulator can be written as:

$$E = E_0 \cos\left(\frac{\varphi(t) + \varphi_0}{2}\right) \cos(\omega t + \frac{\varphi(t) + \varphi_0}{2} + \phi) \quad (1)$$

where  $\omega$  represents the angular frequency of the optical carrier,  $\varphi(t)$  and  $\varphi_0$  represent the optical phase change in the arm of the M-Z modulator stemming from the modulation and DC bias respectively,  $\phi$  is the optical phase delay from the device and  $E_0$  is amplitude of the input field. The first cosine function in equation (1) describes the intensity variation according to the modulation and the second cosine the phase variation under modulation.

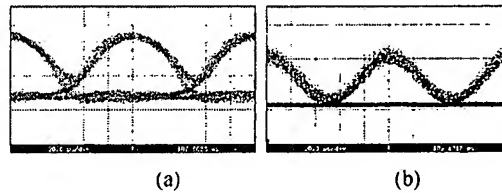


Figure 2: Eye-diagram of electrical (a) and optical (b) RZ signal. 20ps/div.

A maximum phase shift of  $\pi/2$  can be added to the optical signal in this scheme, depending on the modulation voltage of the signal and the switching voltage of the modulator  $V_{\pi}$ . The sign of the chirp can be adjusted by the DC bias. We use an absolute value of phase modulation index of  $0.3\pi$  in our experiment.

### Transmission experiments

In order to investigate the transmission performance of the CRZ pulse, a fibre re-circulating set-up is used as shown in Fig.3.

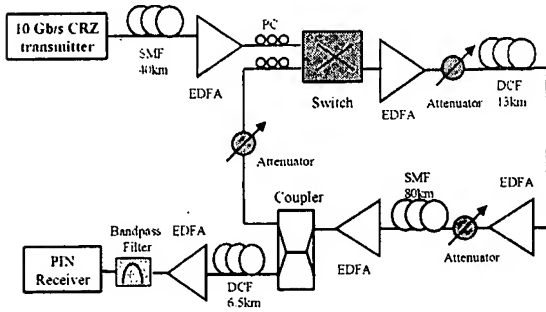


Figure 3: Fibre re-circulating set-up for transmission

The loop contains an 80 km span of SMF and a 13 km dispersion compensating fibre (DCF) providing 100% dispersion compensation. Three commercial EDFAs are used to compensate loss from the SMF, the DCF and the loop switch. Three optical attenuators are used to adjust the power accordingly. The powers into SMF and DCF are optimised at the 45th roundtrip. A 40 km SMF and a corresponding 6.5 km DCF are put after the transmitter and before the receiver, respectively, to reduce the maximum accumulated dispersion in the transmission. A PIN receiver is used and a 1.2 nm optical band pass filter is put before the receiver to reduce the out-of-band ASE noise. BER curves for different transmission distances are shown in Fig.4. from which a 6 dB power penalty at  $\text{BER}=10^{-9}$  can be found after 3600 km transmission.

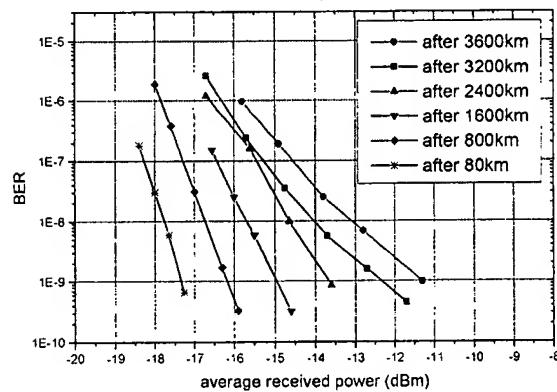


Figure 4: BER curves after transmission

### Discussion

Using the new CRZ transmitter, transmission over 3600 km standard single mode fibre has been achieved. The transmission distance is limited by accumulated ASE noise. The ASE noise accumulation is shown in Fig. 5, where

ASE level is measured after 80 km and 3200 km respectively. This high ASE floor after 3200 km is due to: 1) a long amplifier span of 80 km SMF is used: 2) short loop configuration with only one span of transmission fibre, where one of the 3 EDFAs is used to compensate the loss from the loop switch instead of transmission loss: 3) commercial EDFAs are used in the loop without optimal noise figure.

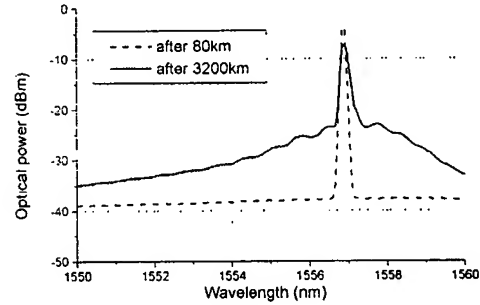


Figure 5: Spectra after 80 km and 3200 km

### Conclusions

A new and simple CRZ transmitter has been proposed and demonstrated using a CW light source and only one external modulator. Transmission over 3600 km SMF has been obtained in a re-circulating loop set-up with 80 km SMF span and full dispersion compensating fibre.

The work is partly supported by the ACTS project DEMON. Authors would like to thank Lucent Technologies Denmark for providing the SMF and DCF fibres.

### Reference

- /1/ E.A. Golovchenko, N.S. Bergano, C.A. Davidson and A.N. Pilipestskii, *Tech. Dig. OFC'1999*, pp246-248.
- /2/ C.R. Davidson, C.J. Chen, M. Nissov, A. Pilipetskii, N. Ramanujam, H.D. Kidorf, B. Pedersen, M.A. Mills, C. Lin, M.I. Hayee, J.X. Cai, A.B. Puc, P.C. Corbett, R. Menges, H. Li, A. Elyamani, C. Rivers and N.S. Bergano, *Tech. Dig. of OFC'2000*, PD25.
- /3/ T. Ito, K. Fukuchi, Y. Inada, T. Tsuzaki, M. Harumoto and M. Kakui, *Tech. Dig. of OFC'2000*, PD24.
- /4/ C. Caspar, H.-M. Foisel, A. Gladisch, N. Hanik, F. Kuppers, R. Ludwig, A. Mattheus, W. Pieper, B. Strebel and H.G. Weber, *IEEE Photon. Technol. Lett.*, 11 (4), 1999, pp481-483.
- /5/ O. Leclerc, P. Brindel, D. Rouvillain, B. Dany, E. Pincemin, E. Desurvire, C. Duchet, A. Shen, F. Blache, F. Devaux, A. Coquelin, M. Goix, S. Bouchoule and P.Nouchi, *Electron. Lett.*, 36(4), 2000, pp337-338.

It Undeliverable Return in ten Days

# AN EQUAL OPPORTUNITY EMPLOYER

OFFICIAL BUSINESS  
PENALTY FOR PRIVATE USE, \$300

